SYSTEM ANALYSIS AND ISOTHERMAL SEPARATE EFFECT EXPERIMENTS OF THE ACCIDENT BEHAVIOR IN PWR SPENT FUEL STORAGE POOLS

H. Chahi[1], W. Kästner[1] and S. Alt[1]

[1]: University of Applied Sciences Zittau/Görlitz, Institute of process technology, process automation and measuring technology, Department of nuclear engineering/Soft computing, Zittau/Germany

[h.chahi, w.kaestner, s.alt]@hszg.de

ABSTRACT

This research project supported by the German Federal Ministry of Education and Research named SINABEL (Safety of spent fuel pools: Experimental analysis, modeling and validation of system and CFD codes) delivers with a combination of experiments and simulations, knowledge's of the heat transfer processes for the case of a partially or completely evaporated spent fuel storage pool in light water reactor nuclear power plants both within the fuel rod bundle of a fuel assembly (FA) and in the spaces between the FA in order to be able to predict via the modeling and simulation the development of the axial and radial temperature profiles of rods by different accident scenarios. SINABEL is a joint research project which three research institutions (TU-Dresden, HZDR and HSZG) work together.

One of the main focus in this project is the investigation of the flow behavior by separate effect experiments in a single 16×16 PWR-FA-dummy (pressurized water reactor fuel assembly) to study the vertical density-driven exchange movements of gases within and above the FA-bundle.

By means of these small scale experiments the flow behavior will be investigated using optical observations facilities for air, replacement atmospheres for superheated steam (e.g. through model fluids). The operational capability is also to be tested as part of this work.

The measuring results in this project include the dynamic behavior of gas concentrations and local velocity vectors, turbulent structures of oppositely directed gas flows.

In this paper the experimental design and results of preliminary isothermal experiments at a shortened PWR-FA-dummy are presented which are based on acquired knowledge's from experiments at a heated BWR-FA-dummy-rig and descriptions of fluid dynamic process in FA. The paper illustrates for example the Re-number dependent pressure drop in FA-dummy and the velocity distribution, as well as determines which model gas is well suited to model the overheated steam by application of simulate principle. The result of the investigation of thermal hydraulic above the FA-dummy (interaction between surrounding environment and gas flow in FA) would be also depicted.

ACKNOWLEDGEMENTS: The project underlying this report is founded by the German Federal Ministry of Education and research (BMBF) under the reference number 02NUK027D (SINABEL). The responsibility for the content of this publication lies with the author.

Keywords: thermal-hydraulic analysis, PWR spent fuel storage pool, separate effect experiment, turbulence, head loss

1. INTRODUCTION

In a research project named SINABEL (security of wet storage facility for spent fuel) new knowledge's of the thermal-hydraulic phenomena in the storage pool are to be acquired. The accident scenarios in a

cooling pool should be replicated using the simulation and modeling. At the project partners TU Dresden, within the scope of project funded at Vattenfall Europe AG, a simulation of the BWR (SVEA-96) with the original size (1: 1) carried out, wherein different accident scenarios were simulated. In the simulation, the rods were heated electrically with different performance and the water and surface temperatures are measured with the thermocouples, which are soldered and positioned at different locations.
In applying of invasive measurement mode is not known whether the temperatures indicated by the thermocouples match the actual temperature in the fluid or the temperature due to the thermal convection in the thermal elements themselves. In this paper, we assume that the displayed values correspond to the temperatures of the surface of the medium (bars) or the fluid. The channel of the fuel assembly was filled in this integral experiment with water before the start of the experiment and the plant was brought up to different performance without filling opportunity with water. Thereby the failure of the cooling process is simulated. The results of the integral experiments (Temperature distribution, steam mass, etc.) flow define the boundary conditions for the investigations with the PWR_FA_Dummy (PWR fuel assembly dummy) presented in this work.

2. SYSTEM MODELLING AND ANALYSIS

Electrically heated rods with various performances simulated BWR-fuel rods in the analyzed experiments. The figure 1 represents the heating rod bundles. The experimental facility is equipped with 24 rods in the inner duct and 4 bars on two sides of the outer channel.
Based on the knowledge acquired from the investigated configuration of BWRs, new knowledge of the flow velocity in the rod bundle and the temporal and spatial temperature distribution are extracted. From the graph 2 witch the steam mass flow described and the known flow cross-section of the inner channel, the flow rate can be calculated with the equation:

$$\boldsymbol{c = \frac{\dot{m}}{\rho A}} \qquad \textbf{Eq. 1}$$

with **c** - the flow velocity, $\boldsymbol{\dot{m}}$ – steam mass flow, $\boldsymbol{\rho}$ – density of steam and A – flow cross section.
From the determined flow rate the dimensionless Reynolds number which describes the ratio of the inertial- to viscous forces, is determined.

$$\boldsymbol{Re = \frac{c.d_H}{\nu}} \qquad \textbf{Eq. 2}$$

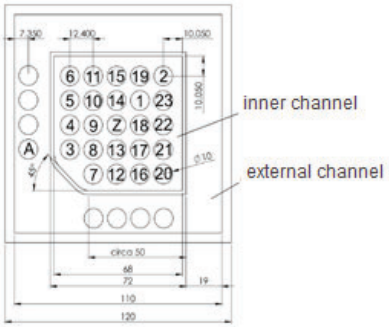

Figure 1 – heating rod bundle SVEA-96 [5]

with c – the flow velocity, d_H – the hydraulic diameter and ν – the kinematic viscosity. For the calculation of the hydraulic diameter the total free surface in the inner channel is taken into account and not the tight cross-section (see figure 1). Witch generally applies:

$$d_H = \frac{4A}{U} \qquad \text{Eq. 3}$$

With U – perimeter and A – flow cross-section

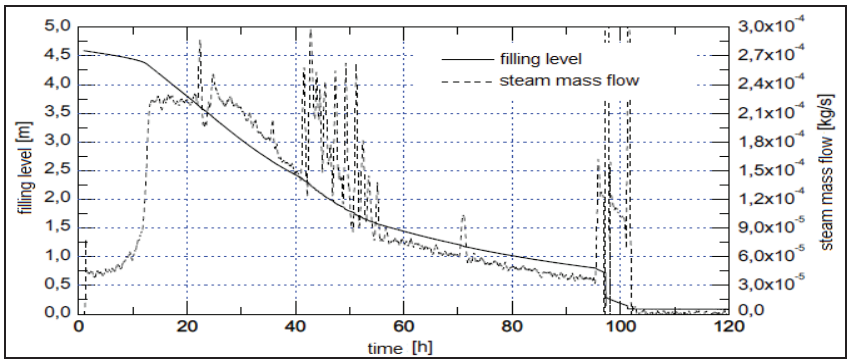

Figure 2 – Steam mass flow by 20 W/Stab and normal pressure [5]

The axial temperature profile, which is shown here only qualitatively, can be seen in figure 3, where the temperature increases with decreasing water level. Once the temperature has reached an extreme value, the temperature decreases due to the inflow of the air within the storage pool. Since the environment has a lower temperature than the temperature of the superheated steam and the surface, while there is a cooling process.

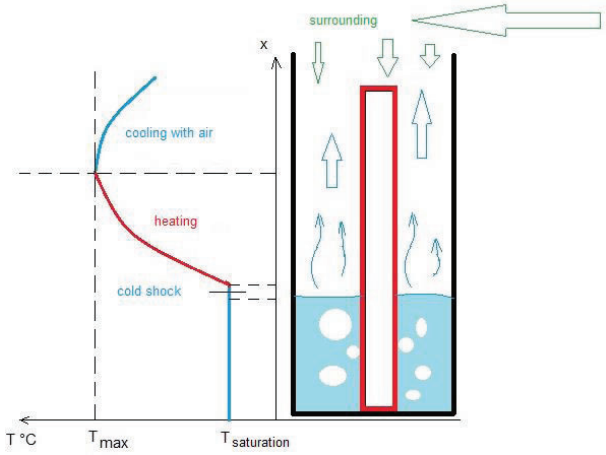

Figure 3 – Qualitative temperature profile in a fuel rod

From the input data of the Table 1, which were taken from the geometry and material data of the water in the experimental conditions, the output data of the modeling have been calculated.

Table 1 – input data for modeling

Input data	value
$\mathbf{d_{st}}$	0,010 m
A	0,00258 m²
$\boldsymbol{\rho^1}$	0,5896 kg/m³
$\dot{m}_{max}$	2,7 kg/s

The output data for modeling are listed in Table 2. With decreasing water level in the integral experiment will determine the flow of steam.

Table 2 – Output data for modeling

Output data	value
A	0,00258 m²
U	1,015 m
d_H	0,0102 m

Since the resulting steam mass flow is variable, which depends on the temperature of the rods, level and material data of the superheated steam, different flow velocities c and Reynolds numbers Re are calculated. The flow rate varies by a factor of the tenth. The dependence of the Reynolds number of the flow velocity is shown in Table 3.

Table 3 – Dependence of Reynolds number from the flow velocity in the integral plant

c in m/s	Re
0,0015	1,1
0,026	18,8
0,034	24,6
0,05	36,2
0,08	57,9
0,1	72,3
0,12	86,8
0,13	94,0

In this consideration and taking into account the fluctuation of the flow rate, a maximum Reynolds number Re = 1000 is to be expected. This means that a laminar flow is present in the rod bundle.

2.1 Gas Model and principle of similarity

Based on the principle of similarity, a model gas is selected in this section. This principle is an important tool to determine the relationship between the parameters that are relevant for the process description, if the experiments with several scales or media would be performed.
Since the vertical exchange movements for the separate-effect experiments not done due to temperature differences between the water vapor (gas) and the atmosphere, but also due to density differences between model gas and atmosphere, the application of the transferability of the results on the basis of similarity considerations is meaningful.
The search for the perfect gas model can come through different criteria about. As an example is to consider the gas density which is used as a criterion of similarity between the real system of the test facility ADELA and the shortened PWR-FA-dummy. For the simulation of similar densities is not possible to use only a gaseous element to model different state of steam. For example, if pure helium gas used as a model, the transferability of the results on the behavior of superheated steam is not ensured, because the density of the steam is much greater than the density of the helium (gaseous at room temperature and normal pressure).
By using of argon under the same conditions the density of this model gas is corresponding to the density of the steam with a moisture content of 36% (1.67 kg / m³). The restriction of experiments on distributed

constant initial densities in the PWR BE dummy is not effective, since in the real process on the one hand, the moisture content in saturated steam parameters conditionally (power, fuel ...) varies and in the upper region of the superheated steam different densities are resulting due to the temperature distribution. For this reason, a height-dependent density distribution with different model gas mixtures (argon, helium) should be given to model the density interval [0.295 kg / m³ to 1.67 kg / m³] of steam under normal pressure, according to the determined experiments conditions at the integral plant. The densities in the range of $0.5896\ kg\ /\ m^3$ to $0.295\ kg\ /\ m^3$ correspond to the temperature of the superheated steam of 100 ° C - 460 ° C at a pressure of 0.1 MPa.

So it is conceivable that e.g. the superheated steam at a temperature 460 ° C (ρ = 0.295 kg / m³) is modeled by a gas mixture of 92.1% and 7.9% and argon -Helium.

$$\boldsymbol{x\rho_{He} + (1-x)\rho_{Ar} = \rho_{\ddot{u}D}} \qquad \textbf{Eq. 4}$$

ρ_G – Density of the corresponding gas G and x- x-gas content of helium.

To ensure physical similarity between the different experiments and the real process, the fulfillment of similarity conditions (geometry and boundary conditions) must always be determined. The separate-effect experiments on PWR-FA-dummy (see Figure 1) provided with the original geometry in the region of the upper spacer and the FA-head, so that the criterion of geometrical similarity at the intersection between FA and located above atmosphere above is fulfilled. Deviating from the original geometry is the shortened length of the existing PWR-FA-dummy which is taken into account. In addition to the density another similarity criteria are conceivable for the transferability of the acquired knowledge from a real process. The advantage of modeling with the dimensionless parameters such as Reynolds number is that the flow behavior can be transmitted through e.g. changing the material properties in different test facility. In the application of Ar-He mixture is taken into account that helium tends to escape.

2.2 Overview of basic data of PWR_FA_Dummy

The DWR_FA_Dummy used by modeling is (pressurized water reactor fuel element dummy) Type Focus 16x16-20-3Sp/ 2Sp with three or two spacers Sp (20 is the number of control rods) and constitutes the basis of the investigations. The figure 4 shows an overview of the basic data of FA_Dummy used.

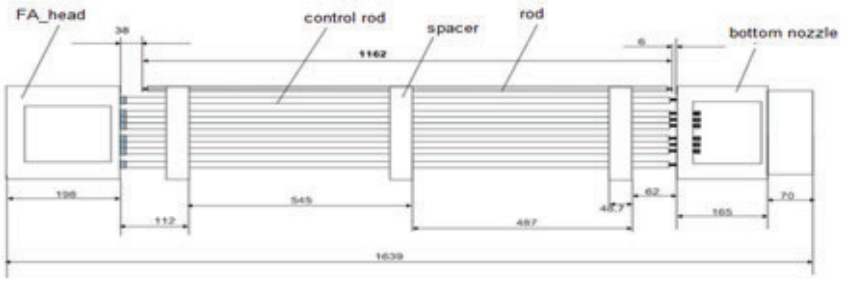

Figure 4 - Length dimensions of the available PWR single-FA-dummy

2.3 Pressure drop by horizontal investigation with air and large Reynolds numbers

On the basis of an air channel, where the Reynolds number can be varied by changing the flow rate or the flow velocity, the static pressure losses were measured in the FA_Dummy. By means of a frequency converter, the frequency of the blower which controlled electric motor is varied. Here we noted that the smallest investigated Reynolds number is Re =537.

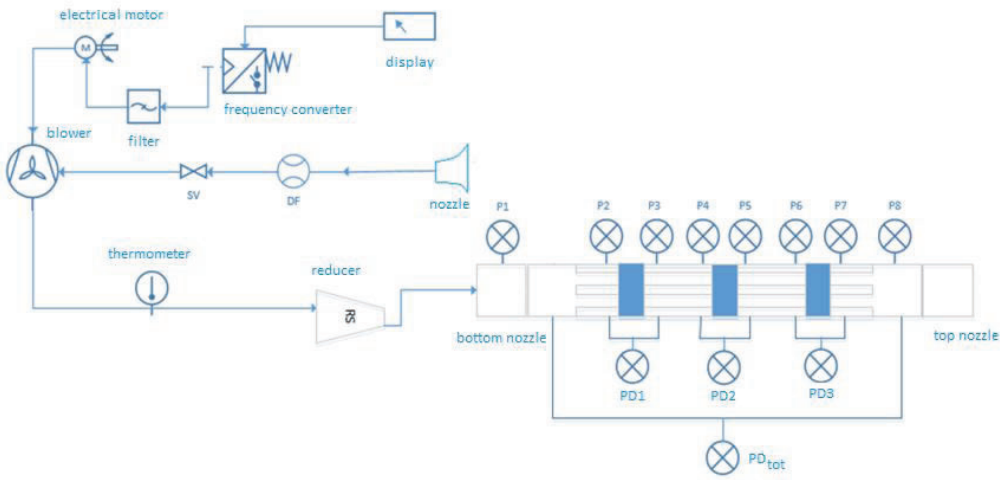

Figure 5 – R & I flow diagram of the experimental facility for measuring the pressure drop with large Reynolds numbers

Figure 6 illustrates the dependence of the pressure drop across the three spacers and across the entire FA-dummy as a function of Reynolds number. It can be clearly seen, that the pressure loss ΔP_i $(i = 1..3)$ is nearly equal at the three spacers. The higher the flow rate or the flow velocity, the greater the pressure drops. Square approaches of compensation curves show good agreement with the measurements.

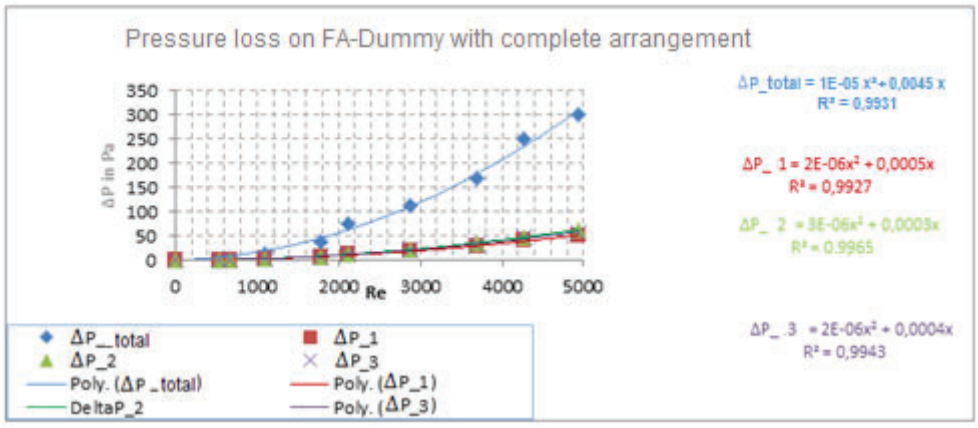

Figure 6 – Pressure losses in FA-Dummy with complete arrangement as a function of Reynolds number

2.4 ζ-value by the horizontal investigation with air and large Reynolds numbers

In this section, the loss coefficients are determined from the measured pressure losses from the test results. Here, a detailed derivation of the calculation of ζ-values is treated for this series of experiments.
Although ultimately the pressure losses occur due to friction, it is divided in pressure drop caused by the friction in the (walls of the housing, rods and spacers) ΔP_R and this due to additional components or deflections occurring pressure drop ΔP_{add}.
This makes the total pressure loss, as follows, illustrated:

$$\Delta \boldsymbol{P_{total}} = \Delta \boldsymbol{P_R} + \Delta \boldsymbol{P_{add}} \qquad \textbf{Eq. 5}$$

The calculation of the wall friction is given by:

$$\Delta P_R = \lambda \frac{l}{d_H} \left(\frac{1}{2} \rho c^2\right) \qquad \textbf{Eq. 6}$$

with λ friction coefficient, ρ density, c velocity, l total length und d_H hydraulic diameter.

The so-called dynamic pressure can be determined by the Eq.7.

$$p_s = \frac{1}{2} \rho c^2 \qquad \textbf{Eq. 7}$$

The second pressure loss component ΔP_{Zus} combines all the parameters that cause the loss of pressure but not analytically definable. From all this unknown parameters results the dimensionless number, so-called pressure loss coefficient ζ or form drag.
It follows that:

$$\Delta P_{add} = \zeta \left(\frac{1}{2} \rho c^2\right) \qquad \textbf{Eq. 8}$$

Through a series circuit of several installations, the pressure losses for the total flow path can be added. Provided that the components doesn't interfere with each other. This means that enough distance exists between the internals, witch the flow neutralizes. In laminar flow, the friction factor λ depends on the Reynolds number Re, as follows:

$$\lambda = \frac{\mathrm{k}}{\mathrm{Re}} \qquad \textbf{Eq. 9}$$

Where k = 64 is to be expected in the case of laminar flow in smooth tube. After transposing the equation 1 to the variable c

$$c = \frac{Re.\nu}{d_H} \qquad \textbf{Eq. 10}$$

and from Eq. 6 and Eq. 9 the pressure loss ΔP_R is defined as:

$$\Delta P_R = \frac{k}{Re} \frac{l}{d_H} \left[\frac{1}{2} \rho \left(\frac{Re.\nu}{d_H}\right)^2\right] \qquad \textbf{Eq. 11}$$

After simplifying the equation Eq. 11, it turns out that the pressure loss ΔP_R is directly proportional to Re.

$$\Delta \mathrm{P_R} = \underbrace{\frac{\mathrm{kl\rho\nu^2}}{\mathrm{2{d_H}^3}}}_{\mathrm{b}} \mathrm{Re} \qquad \textbf{Eq. 12}$$

Instead, the pressure drop ΔP_{add} is directly proportional to Re^2.

$$\Delta P_{add} = \zeta \left(\frac{1}{2} \rho \left(\frac{Re.\nu}{d_H}\right)^2\right) \qquad \textbf{Eq. 13}$$

This means:

$$\Delta P_{add} = \underbrace{\frac{1}{2} \frac{\zeta \rho \nu^2}{{d_H}^2}}_{a} Re^2 \qquad \textbf{Eq. 14}$$

From the pressure drop diagrams and correlation, the constant a and b can be determined. Thus, the pressure loss between the spacer Sp1 ($\boldsymbol{\Delta P\_1}$) for example is described by the equation:

$$\boldsymbol{\Delta P\_1} = \underbrace{\mathbf{2 \times 10^{-6}}}_{a}\ \boldsymbol{Re^2} + \underbrace{\mathbf{0,0005}}_{b}\ \boldsymbol{Re} \qquad \textbf{Eq. 15}$$

From the detected values (a and b) the values ζ and k are determined.

Table 4 – Material properties and geometry data to determine the pressure loss coefficients

	Value
density $\boldsymbol{\rho}$	1,14 kg/m³
kinematic viscosity ν	$1{,}58 \times 10^{-5}$ m²/s
hydraulic diameter d_H	0,0116 m
related length l	0,1 m

Table 4 shows material properties and geometry data that are relevant for calculating of the pressure drop coefficients. After transposing the equation and some simplifications:

$$\boldsymbol{b} = \frac{\boldsymbol{kl\rho\nu^2}}{\mathbf{2}\boldsymbol{d_H}^3} \qquad \textbf{Eq. 16}$$

and

$$\mathbf{a} = \frac{\mathbf{1}}{\mathbf{2}}\frac{\boldsymbol{\zeta}\boldsymbol{\rho}\boldsymbol{\nu}^2}{\mathbf{d_H}^2} \qquad \textbf{Eq. 17}$$

we obtain

$$\mathbf{k} = \frac{\mathbf{2b}\mathbf{d_H}^3}{\mathbf{l}\boldsymbol{\rho}\boldsymbol{\nu}^2} \qquad \textbf{Eq. 18}$$

$$\boldsymbol{\zeta} = \mathbf{2}\frac{\boldsymbol{a}\boldsymbol{d_H}^2}{\boldsymbol{\rho}\boldsymbol{\nu}^2} \qquad \textbf{Eq. 19}$$

The total pressure loss coefficient is determined from the ζ value and the pipe friction coefficient.

$$\boldsymbol{\zeta_{total}} = \boldsymbol{\zeta} + \underbrace{\frac{\mathbf{k}}{\mathbf{Re}}}_{\boldsymbol{\lambda}} \times \frac{\mathbf{l}}{\mathbf{d_H}} \qquad \textbf{Eq. 20}$$

According to Table 4, Eq.18 and Eq.19 and Figure 8 the following values are determined by horizontal studies with large Reynolds number.

Table 5 - Loss coefficients for the three spacers in the BE dummy

	Sp1	**Sp2**	**Sp3**	**mean**
ζ	1,89	2,84	1,89	2,20
k	54,85	32,91	43,88	43,88

Figure 7 shows graphically the calculated friction coefficients for the three spacers of the FA_Dummy.

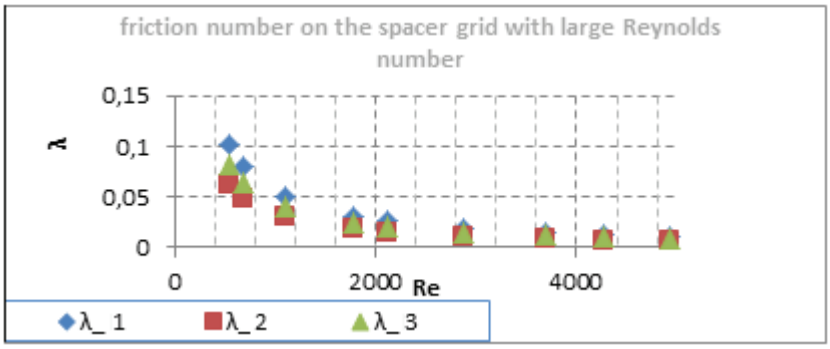

Figure 7 – friction number on the spacers with large Reynolds number (SG, bars and wall)

In order to consider precisely the influence of the spacers, the resulting pressure losses (a see Figure 8)) are eliminated from the measured pressure difference (due to the walls of the housing and the bars) between the spacer (see Figure 8 b). For this purpose two measuring points are chosen, between which no additional components are installed. The pressure difference (continuous pressure losses) is only dependent on the wall friction (tube - wall).
From the constant b of Figure 8a and the equation Eq. 18 the K-value (k = 152) is calculated. Furthermore, a K-value (k = 32.91) and ζ-value (ζ = 1.89) are determined from the quadratic function from Figure 8b. The new calculated K-value for the Spacer agrees with the value determined from the table 5. While the friction coefficient by Kakaç describes the pressure loss caused by rods the at narrow cross section, the calculated friction coefficients for small and large Reynolds numbers refer to the total free surface (see Figure 3).

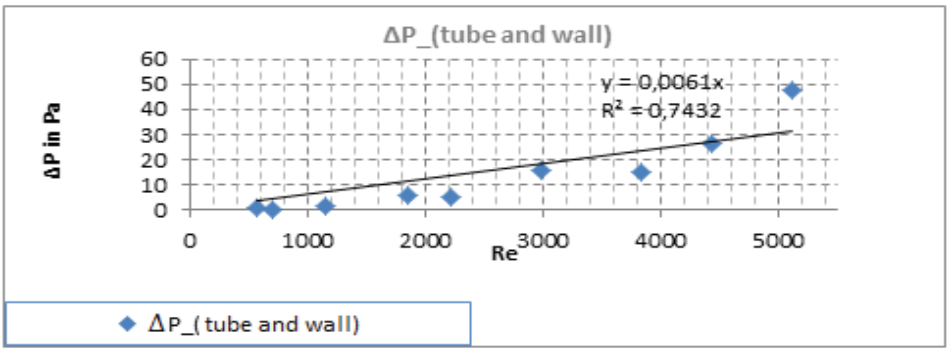

a)

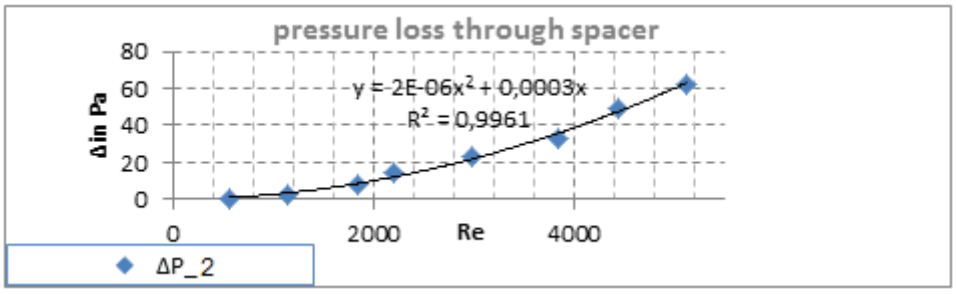

b)

Figure 8 – Pressure drop through a) the walls and tube, b) spacer grid

2.5 Test results with air for small Reynolds numbers

In order to investigate the low range of Reynolds numbers a test facility was constructed. In these experiments, the backlash, which was detected by the CFD calculations by the project partner, was taken into account.
Figure 9 shows the R & I flow diagram of the test stand. The investigated FA-Dummy has 3 Spacers (16x16-20-3Sp).

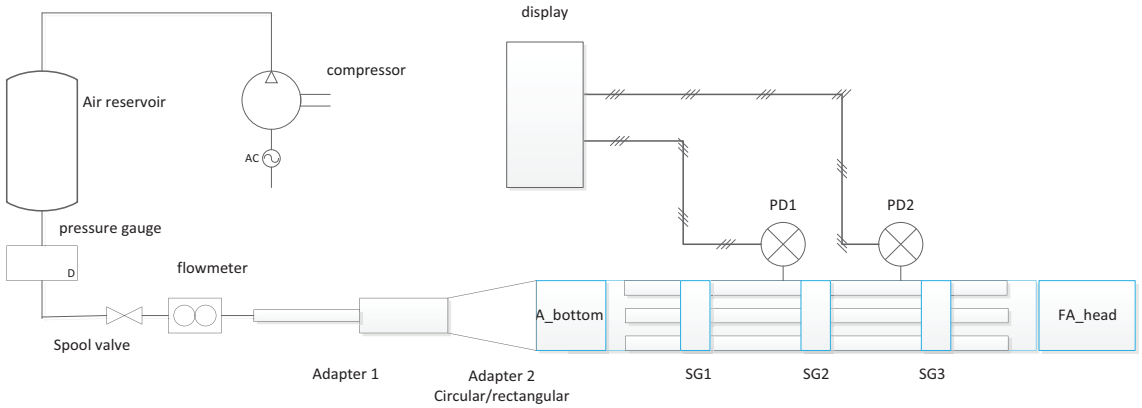

Figure 9 – R & I flow diagram of the experimental system for measuring the pressure losses with very small Reynolds numbers

In this series of experiments, the pressure drop across the second spacer was measured for quasi-constant pressure. This means that the volume flow, which is measured by the digital tachometer, is not brought to the target value on the basis of an automatic controller, but by the manual adjustment of the valve.

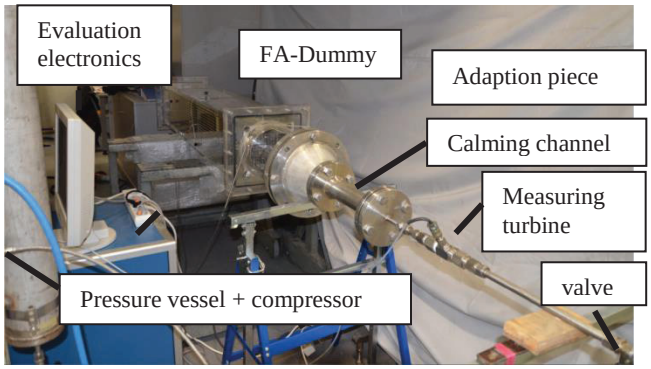

Figure 10 – Experimental facility for horizontal investigations with air for small Reynolds numbers

Since the flow velocities are very low, results a time lag between the determined pressure differences and the set flow rate taking into account the distance between the digital speedometer and the measuring points. In order to eliminate this problem, the average of the calculated values was calculated for a given flow rate. In this case, the distance between the measuring points is in consideration of the backlash 540 mm.

The Figure 11 shows the pressure drop and the pressure drop per unit length of the horizontal investigations with air as the gas model for very low flow rates.

$$\Delta P_{lenght} = \frac{\Delta P}{l} \qquad \textbf{Eq. 21}$$

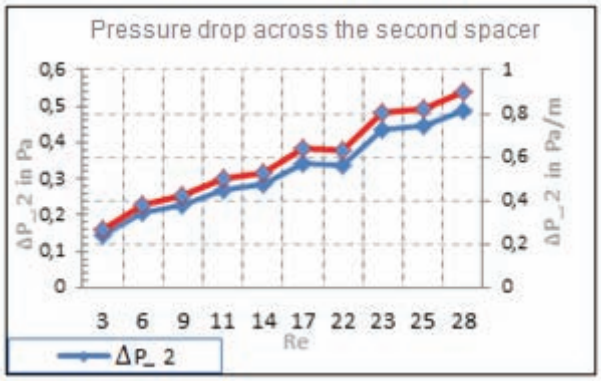

Figure 11 – Pressure drop across the second spacer with quasi-constant volume flow

Furthermore, the pressure loss was measured with decreasing pressure, the pressure vessel with air (8 bar pressure) was charged and the air was dismissed by a shut-off valve. The test results are shown in Figure 12.

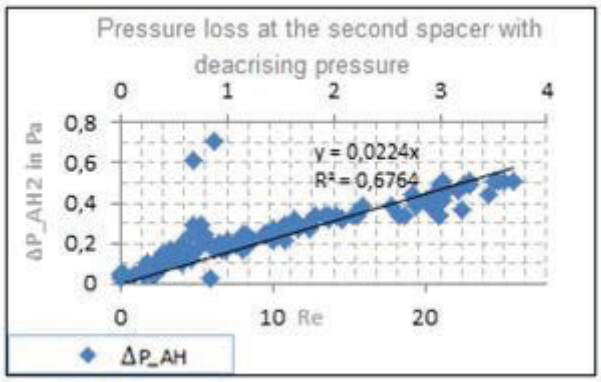

Figure 12 – Pressure loss at the second spacer with decreasing pressure

In determining the pipe friction factor for small Reynolds numbers the ζ-value, which is calculated from the previous analysis for the second spacer (see Table 3), is considered. The pressure loss caused due to the components is calculated from the measured pressure drop and the corresponding length is subtracted (taking into account the backlash). In the literature, the geometric factors for the narrow cross-sections of different configuration were investigated. For the configuration investigated, the ratio of the FA_Dummy pitch_to_diameter is P / D = 1.419. The acquired correlation from the measurement series was defined in Kakaç [3] with the equation:

$$\boldsymbol{fRe = 40,7(\frac{P}{D} - 1)^{0,435}} \qquad \textbf{Eq. 22}$$

Using the equation (Eq. 22) the geometry factor is by Kakaç fRe = 27,88. Based on the Governing equation in the cylindrical coordinates and the numerical solution of the Laplace equation, Sparrow & Löffler [4] defined the correlation according to the equation Eq. 23 in the case of an axial laminar flow between the square-mounted tubes.

$$\boldsymbol{fRe = \frac{8(1-\varepsilon^*)^2}{2\varepsilon^* - ln\varepsilon^* - 0,5(\varepsilon^*)^2 - 1,5}} \qquad \textbf{Eq. 23}$$

with

$$\varepsilon^* = 1 - P/d \qquad \text{Eq. 24}$$

The K-value for this correlation is $(k = 20{,}46)$. From the constant k, which is determined by experimental investigations with high Reynolds numbers (see Table 3), the pipe friction coefficients is calculated even for small Reynolds numbers with the equation Eq. 18. The Figure 13 shows the test results for the friction coefficient with air that flows as a medium for small Reynolds numbers.

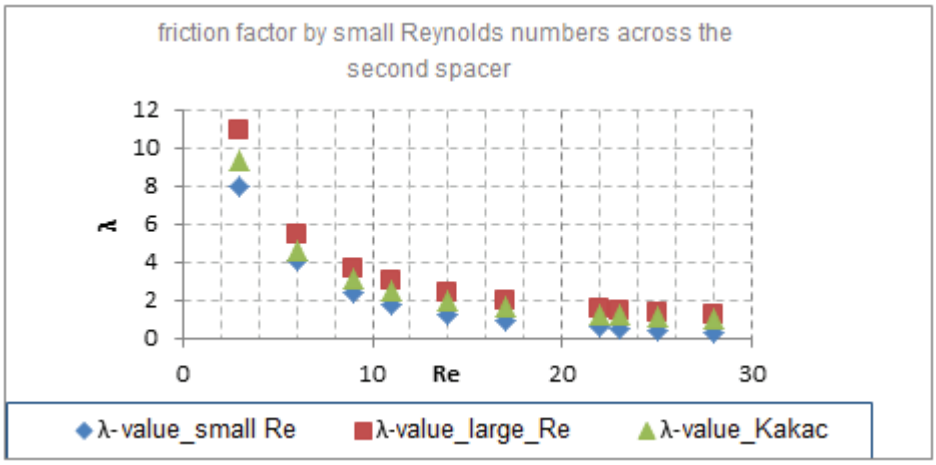

Figure 13 – Comparison of friction factors

2.6 Flow velocity by horizontal investigation with air

To measure the local flow velocity in a 16x16 Bundle a Prandtl-tube was used. The Figure 14 represents the measuring point by determining the local velocity in the horizontal investigations with air for small Reynolds numbers.

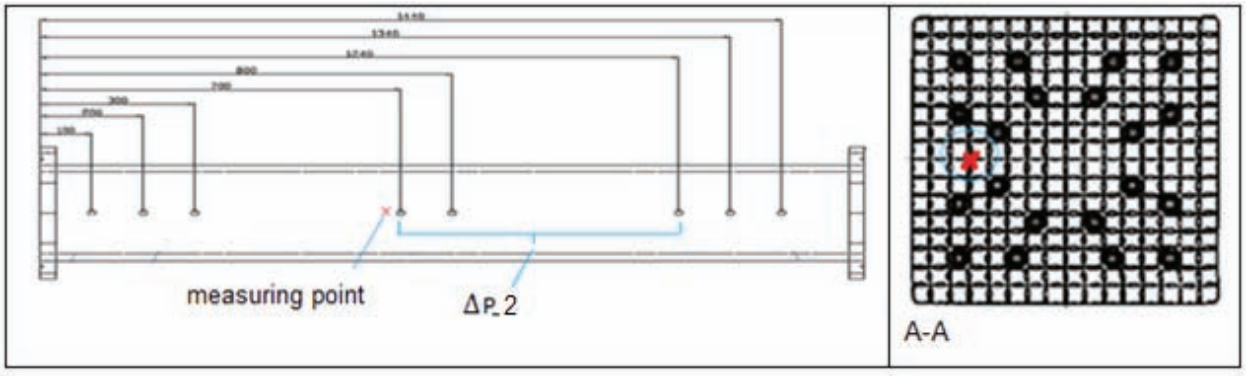

Figure 14 – Measuring point to determine the local and average flow velocity

The dynamic pressure is calculated as difference of total pressure that is measured by the Pitot tube and the static pressure according to the equation.

$$P_{dyn} = P_{total} - P_{sta} \qquad \text{Eq. 25}$$

From the dynamic pressure, the local flow rate to be measured:

$$c_{lokal} = \sqrt{\frac{2P_{dyn}}{\rho_{Luft}}} \qquad \text{Eq. 26}$$

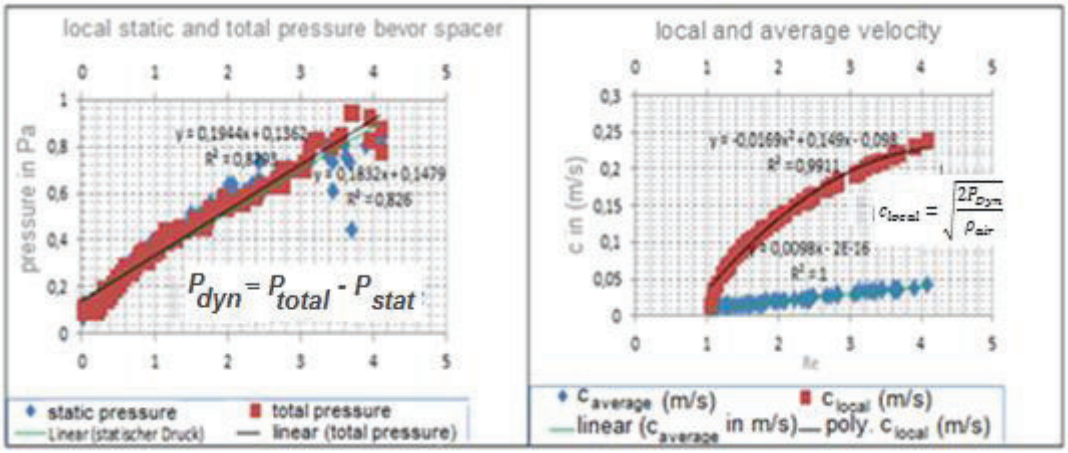

Figure 15 – Comparison of measured local and average flow velocity

3. CONCLUSION

The determination of the thermo-hydraulic design parameters for gas model was performed on the basis of similarity analyzes to ensure the transferability of the conditions for steam development in the PWR FA-dummy on the model gases. In particular, the Reynolds number is the basis for selection of the gas model to simulate the exchange of vertical movement.
The isothermal flow experiments with the PWR fuel element (FA)-dummy "type Focus 16 × 16-20 with three spacers (Sp), FA-top-nozzle and bottom" for various Reynolds (Re) numbers are carried out. The aim of the preliminary experiments is to determine flow-relevant parameters for the modeling, such as loss coefficients and pipe friction factors, and compared with the literature data, since it is necessary to know the geometric properties of the used PWR-FA-dummy and its impact on the flow already when creating the grid mesh. Furthermore, it is helpful by modelling to acquire knowledge of the properties of flow influencing local discontinuities in the flow direction, such as the spacer (Sp).
In the investigations with small Reynolds numbers, the local flow velocity was measured at the center of a non-influenced control rod guide tubes cooling channel between the fuel rods by means of an invasive measuring method (Pitot tube).

Nomenclature

A	flow area
Ar	argon gas
BWR	boiling water reactor
c	velocity
c_{local}	local velocity
$c_{mittlere}$	average velocity
D	diameter
d_H	hydraulic diameter
FA	fuel assembly
f	friction factor
He	helium

K	constant
l	length
$\dot{m}$	mass flow
P	pitch
P	pressure
PD	pressure difference device
P_{add}	Pressure drop due to additional components
P_{dyn}	dynamic pressure
P_s	static pressure
P_{total}	total pressure
PWR	pressurized water reactor
Re	Reynolds number
Sp	spacer
ζ	pressure loss coefficient
Δ	difference
ν	kinematic viscosity
λ	friction factor
ρ	density

REFERENCES

[1] Tae-Hyun CHUN ;t and Dong-Seok OH, "*Pressure Drop Model for Spacer Grids with and without Flow Mixing Vanes*", Advanced Reactor Development, Korea Atomic Energy Research Institute, (May 11, 1998)

[2] K. Rehme, G. TRIPPE, "*PRESSURE DROP AND VELOCITY DISTRIBUTION IN ROD BUNDLES WITH SPACER GRIDS*", Kernforschungszentrum Karlsruhe-Institut far Neutronenphysik und Reaktortechnik BUNDLES WITH SPACER GRIDS, Juli 1979

[3] S. Kakac, K. Shah, W. Aung, " *HANDBOOK OF SINGLE- PHASE CONVECTIVE HEAT TRANSFER*", Wiley Interscience Publication, 1987

[4] E. M. Sparrow, A. L. Löffler, "*Longitudinal Laminar Flow Between Cylinders Arranged in Regular Array*", National Aeronautics and Space Administration, Lewis Research Center, Cleveland, Ohio, September 1959

[5] S. Schulz, C. Schuster and A. Hurtado, "*EXPERIMENTAL INVESTIGATION OF BOIL-OFF-SCENARIO IN BWR SPENT FUEL POOLS"*, Technische Universität Dresden, Institute of Power Engineering, ICONE21-16830